

Exploring integrability-chaos transition with a sequence of independent perturbations

Vladimir A. Yurovsky

School of Chemistry, Tel Aviv University, 6997801 Tel Aviv, Israel

A gas of interacting particles is a paradigmatic example of chaotic systems. It is shown here that even if all but one particle are fixed in generic positions, the excited states of the moving particle are chaotic. They are characterized by the number of principal components (NPC) — the number of integrable system eigenstates involved into the non-integrable one, which increases linearly with the number of scatterers. This rule is a particular case of the general effect of an additional perturbation on the system chaotic properties. The perturbation independence criteria ensuring the system chaoticity increase are derived here as well. The effect can be observed in experiments with photons or cold atoms as the decay of observable fluctuation variance, which is inversely proportional to NPC, and, therefore, to the number of scatterers. This decay indicates the approaching of the eigenstate thermalization. The results are confirmed by numerical calculations for a harmonic waveguide with zero-range scatterers along its axis.

Evolution of integrable systems is completely predictable and, according to the Kolmogorov-Arnold-Moser theorem, weak perturbations do not affect this property. There are numerous examples of such classical and quantum systems, including stellar mechanics, hydrogen atoms, and many-body systems, both realized in experiments, such as quantum Newton cradle [1, 2] and cold-atom breathers [3, 4] (see [5–8] for the theoretical description) and those waiting for the realization [9].

When the integrability-lifting perturbation is sufficiently strong, the system evolution becomes unpredictable. Nevertheless, a completely-chaotic system relaxes to a state described by the Gibbs ensemble, thanks to the eigenstate thermalization mechanism — eigenstate expectation values are equal to microcanonical averages at the eigenstate energy — introduced in [10, 11] (see also [12, 13], the experimental work [14], the review [15] and the references therein). In contrast, integrable systems relax to states described by the generalized Gibbs ensemble [16–20].

However, a general system lies between integrable and completely-chaotic systems [21–43]. Chaoticity of such incompletely-chaotic systems can be characterized by the inverse participation ratio (IPR) [24, 27, 29, 44]. Its inverse — the number of principal components (NPC) — estimates the number of integrable system eigenstates comprising the non-integrable one. IPR ranges from 1 for integrable systems to 0 for completely-chaotic ones. It governs the expectation values after relaxation in incompletely-chaotic systems with no selection rules [24, 27]. This regularity has been confirmed in different systems [37]. The fluctuations of expectation values over eigenstates are strong for integrable systems and vanish in completely-chaotic ones, according to the eigenstate thermalization hypothesis. These fluctuations, too, are governed by IPR [28].

Exploration of the integrability – eigenstate thermalization crossover is of special interest, and the means of the system chaoticity prediction based on its Hamiltonian, with no numerical calculations, would be very

useful. The exponential decay of fluctuations in many-body systems with the number of particles was predicted in [11]. However, this sharp decay complicates the exploration. Analytical predictions for single particles with random-matrix perturbations (see [27] and the references therein) are applicable to strong perturbations (and chaos) only. The system chaoticity can be modified by an additional perturbation, e.g., it can lift integrability, transforming an integrable system into a chaotic one. However, the effect of an additional perturbation on a chaotic system is ambiguous, e.g., the system integrability can be restored if the additional perturbation cancels the integrability-lifting one. The perturbation independence criteria, ensuring the system chaoticity increase due to an additional perturbation, are determined here. Then, a linear increase of NPC with the number of independent perturbations of the same shape is predicted. Simultaneous decay of expectation value fluctuations indicates the approaching of the eigenstate thermalization. These predictions are confirmed by numerical calculations for a harmonic waveguide with zero-range scatterers along its axis.

Consider a sequence of Hamiltonians $\hat{H}_s = \hat{H}_0 + \sum_{s'=1}^s \hat{V}_{s'}$. Here, the integrable one \hat{H}_0 has the eigenstates $|\mathbf{n}\rangle$ and eigenenergies $E_{\mathbf{n}}$ labeled by a proper set of integrals of motion \mathbf{n} . The integrability is lifted by the perturbations $\hat{V}_{s'}$. The eigenstates $|\alpha_s\rangle$ of the non-integrable Hamiltonians \hat{H}_s are labeled in the increasing order of their eigenenergies E_{α_s} . Each eigenstate $|\alpha_s\rangle$ can be expanded in terms of $|\mathbf{n}\rangle$, and the strength function

$$W_s(E_{\mathbf{n}}, E_{\alpha_s}) = \left\langle |\langle \mathbf{n} | \alpha_s \rangle|^2 \right\rangle \quad (1)$$

is the probability averaged over states with a fixed energy difference (see [45]). The relation between the strength functions for $|\alpha_s\rangle$ and $|\alpha_{s-1}\rangle$

$$W_s(E_{\mathbf{n}}, E_{\alpha_s}) \approx \sum_{E_{\alpha_{s-1}}} W_{s-1}(E_{\mathbf{n}}, E_{\alpha_{s-1}}) \left\langle |\langle \alpha_{s-1} | \alpha_s \rangle|^2 \right\rangle \quad (2)$$

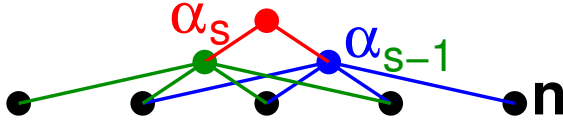


Figure 1. A chart of connection between eigenstates. The number of the integrable system eigenstates \mathbf{n} connected to the non-integrable ones increases from 4 to 5 due to an additional perturbation.

is obtained (see [45]) neglecting the interference terms. This approximation is applicable whenever the perturbation \hat{V}_s is independent of $\hat{V}_{s'}$ with $s' < s$, i.e.,

$$\sum_{\mathbf{n}, \mathbf{n}'} \langle \mathbf{n} | \hat{V}_s | \mathbf{n}' \rangle \langle \mathbf{n}' | \hat{V}_{s'} | \mathbf{n} \rangle \ll \sum_{s''} \sum_{\mathbf{n}, \mathbf{n}'} \left| \langle \mathbf{n} | \hat{V}_{s''} | \mathbf{n}' \rangle \right|^2. \quad (3)$$

The summations over \mathbf{n} and \mathbf{n}' in the microcanonical interval (see [45]) lead to the Berry autocorrelation function [46]. It is localized within the characteristic de Broglie wavelength determined by the characteristic eigenstate energy. Condition (3) is satisfied, for example by coordinate-dependent potentials which have different parity or rotation symmetry, or if the spatial separation between local potentials exceeds the characteristic de Broglie wavelength.

The relation (2) means that an addition of an independent perturbation increases the number of the integrable system eigenstates involved to the non-integrable one (see Fig. 1). This intuitive picture illustrates the recurrent relation for NPC η_s^{-1} (where $\eta_s \equiv \sum_{\mathbf{n}} |\langle \alpha_s | \mathbf{n} \rangle|^4$ is IPR)

$$\eta_s^{-1} = \eta_{s-1}^{-1} + \nu. \quad (4)$$

The parameter ν is approximately independent of s if the chaotic properties of $|\alpha_s\rangle$ weakly depend on s and the shape of \hat{V}_s is independent of s (as for scatterers with the same strength). Then (4) provides a linear dependence $\eta_s^{-1} = \eta_2^{-1} + (s-2)\nu$ of NPC on the number of scatterers.

The relation (4) is derived in [45] using the Lorentzian profile

$$W_L(E, \Gamma) = \frac{1}{\pi} \frac{\Gamma}{E^2 + \Gamma^2} \quad (5)$$

for the continuous strength function $W_s(E_{\mathbf{n}}, E_{\alpha_s}) \approx W_L(E_{\alpha_s} - E_{\mathbf{n}}, \Gamma_s) \Delta E$. Here ΔE is the average difference between eigenenergies in the vicinity of E_{α} . Since $W_s(E_{\mathbf{n}}, E_{\alpha_s})$ should decay as $(E_{\mathbf{n}} - E_{\alpha_s})^{-2}$ in the limit $|E_{\mathbf{n}} - E_{\alpha_s}| \rightarrow \infty$, (see [45]) but has no singularities as $E_{\mathbf{n}}$ and E_{α_s} never coincide, this profile is a natural choice for the strength function. Such strength function has been applied to systems with strong random-matrix perturbations [27, 47–50], when the profile contains many energy levels and Γ can be evaluated using the Fermi golden rule. On the integrability-chaos crossover,

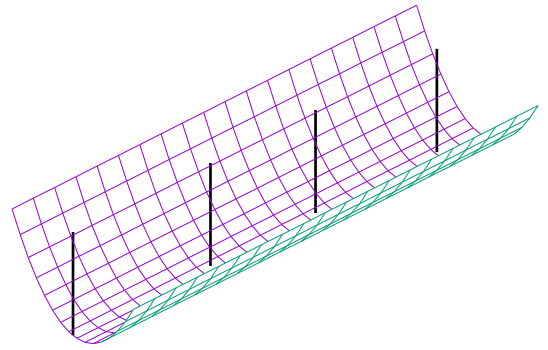


Figure 2. Harmonic waveguide with four zero-range scatterers along its axis

explored here, the profile may contain only few levels and the Fermi golden rule can be inapplicable, but the strength function with some Γ retains the necessary properties.

The prediction (4) is tested for models where the integrability of a particle in a potential with separable coordinates is lifted by s fixed zero-range scatterers. Other examples of such models are flat orthogonal billiards — multiscatterer generalizations of the Seba billiard [51]. Their energy spectrum properties were analyzed for up to 6 scatterers [52–54]. Scattering in a harmonic potential was analyzed in [55]. The set of scatterers is a particular case of the rank- s separable potential $\hat{V}_{s'} = V_{s'} |\mathcal{F}_{s'}\rangle \langle \mathcal{F}_{s'}|$ with the formfactors $|\mathcal{F}_{s'}\rangle$. For such potentials the eigenstate expansion coefficients can be expressed as

$$\langle \mathbf{n} | \alpha_s \rangle = \sum_{s'=1}^s V_{s'} \frac{\langle \mathbf{n} | \mathcal{F}_{s'} \rangle \langle \mathcal{F}_{s'} | \alpha_s \rangle}{E_{\alpha_s} - E_{\mathbf{n}}}$$

in terms of s overlaps $\langle \mathcal{F}_{s'} | \alpha_s \rangle$ which obey the set of linear equations

$$\sum_{s'=1}^s \left(V_{s'} \sum_{\mathbf{n}} \frac{\langle \mathcal{F}_{s''} | \mathbf{n} \rangle \langle \mathbf{n} | \mathcal{F}_{s'} \rangle}{E_{\alpha_s} - E_{\mathbf{n}}} - \delta_{s''s'} \right) \langle \mathcal{F}_{s'} | \alpha_s \rangle = 0. \quad (6)$$

Separable potentials can also approximate long-range, e.g., dipole-dipole ones [56].

The present models are generalizations of the single-scatterer model [22–25]. The integrable Hamiltonian contains the kinetic energy and the radial harmonic potential with the frequency ω_{\perp} ,

$$\hat{H}_0 = \frac{\hbar^2}{2m} \left[\left(\frac{1}{i} \frac{\partial}{\partial z} - A \right)^2 - \Delta_{\rho} \right] + \frac{m\omega_{\perp}^2 \rho^2}{2},$$

where z and ρ are the axial and radial coordinates, respectively, m is the particle mass, and A is a vector potential. The discrete energy spectrum is provided either by the periodic boundary conditions (PBC), $\langle z + L | \alpha_s \rangle = \langle z | \alpha_s \rangle$, or by a hard-wall box, $\langle z = 0 | \alpha_s \rangle =$

$\langle z = L | \alpha_s \rangle = 0$. The formfactors of the separable perturbation are $\langle \mathbf{r} | \mathcal{F}_{s'} \rangle = \delta_{\text{reg}}(\mathbf{r} - \mathbf{R}_{s'})$, where $\delta_{\text{reg}}(\mathbf{r})$ is the Fermi-Huang pseudopotential, and the scatterer position $\mathbf{R}_{s'} = (0, 0, z_{s'})$ has the zero radial component (see Fig. 2). The Hamiltonian \hat{H} is rotationally symmetric along the waveguide axis and the perturbation affects only the states with zero angular momentum. Then, only products $|nl\rangle$ of the axially symmetric wave function $|n\rangle$ of two-dimensional harmonic oscillator and a plane wave with the momentum $2\pi\hbar l/L$ are considered here. They have the eigenenergies $E_{nl} = 2\hbar\omega_{\perp}n + \hbar^2(2\pi l/L - A)^2/(2m)$.

Unlike a flat billiard with a constant energy density of states, in the present model $E_{\alpha} \propto \alpha^{2/3}$, as for a three-dimensional free particle, and the energy density of states $\partial\alpha/E_{\alpha} \propto E_{\alpha}^{1/2}$ increases with the energy. The logarithmic asymptotic freedom [52] found for flat billiards is related to decreasing effective coupling $V_{\text{eff}} \propto 1/\log E$. However, it is a specific property of the systems with $E_{\alpha} \propto \alpha$. If $E_{\alpha} \propto \alpha^{\gamma} (\gamma \neq 1)$, one can see from the derivation [52] that $V_{\text{eff}} \propto E^{1-1/\gamma}$ has the same energy dependence as the energy difference between the states $\partial E_{\alpha}/\partial\alpha \propto E^{1-1/\gamma}$. Then, the present model, as well as a generic system with $\gamma \neq 1$, does not show the asymptotic freedom.

In the absence of the vector potential, $A = 0$, the energy spectrum of the integrable Hamiltonian is degenerate, $E_{nl} = E_{n-l}$. The degeneracy will be lifted by any potential with undefined parity. The vector potential lifts it as well, with no complication of the wavefunctions. However, the Hamiltonian loses the time reversal (T) invariance.

Four models are considered here. The non-symmetric model is T-noninvariant and the scatterer positions $z_1 = 0$, $z_{s'} = (s' - 1 + \delta_{s'})L/s$ ($s' > 1$) have no symmetry due to random shifts $-0.25 \leq \delta_{s'} < 0.25$ chosen once for each s . The symmetric model with $z_{s-s'+1} = z_s - z_{s'}$ and equal $V_{s'}$ is PT-invariant, where P is the inversion over $z_s/2$. The T-invariant model has $A = 0$ and the same scatterer positions as the non-symmetric one. Only this model has degenerate E_{nl} . The three previous models correspond to PBC, while the fourth, box, model, corresponds to the hard-wall box, has $A = 0$, and $z_{s'} = (s' + \delta_{s'})L/(s + 1)$.

Since $\langle \mathcal{F}_{s'} | nl \rangle \langle nl | \mathcal{F}_{s'} \rangle \propto \exp(2i\pi l(z_{s''} - z_{s'})/L)$ for PBC, summation over l in (6) can be done analytically like in [22], leaving a sum over $\sim E_{\alpha}/\omega_{\perp}$ values of n (the closed-channel contributions with $n\omega_{\perp} > E_{\alpha}$ decay exponentially with n). Similar summation can be done for the hard-well box too. As $E_{\alpha} \propto \alpha^{2/3}$, calculation of the system (6) matrix and its solution require $\sim s^2\alpha^{2/3}$ and $\sim s^3$ operations, respectively. Then α eigenstates are calculated for $\alpha \gg s^{3/2}$ with $\sim s^2\alpha^{5/3}$ operations (cf. with $\sim \alpha^3$ operations required by the direct diagonalization method).

The plots of NPC (see Fig. 3) as a function of the number of scatterers for the four models confirm the

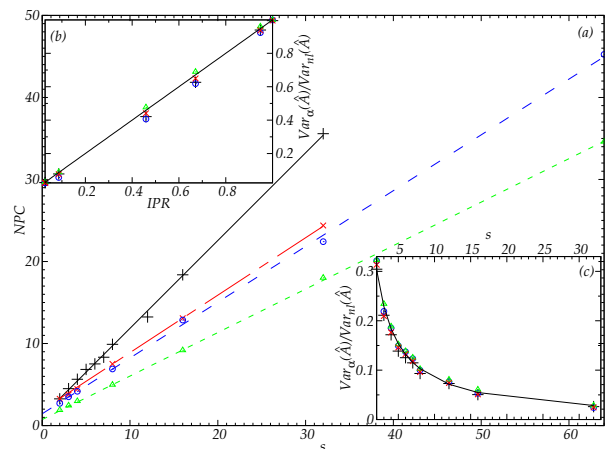


Figure 3. (a) The dependence of the number of principal components on the number of scatterers for the non-symmetric (pluses), symmetric (crosses), box (circles), and time-reversible (triangles) models in the unitary regime of strong perturbations. The lines represent the linear fits. (b) The ratio of variances over eigenstates of the non-symmetric model with 32 scatterers to ones of the integrable system as a function of the inverse participation ratio on the change of the perturbation strength from the unitary regime to zero. (c) The same ratio as a function of the number of scatterers in the unitary regime. In (b) and (c), the symbols represent four observables, namely, the axial momentum (crosses), the part of the transverse potential energy in the total energy (pluses), and the occupations of the positive momenta (triangles) and of the odd axial modes (circles). The lines show IPR.

linear dependence (4). The linear fits have two model-dependent parameters: η_2 , which cannot be predicted by (4) since the system with a single scatterer is not chaotic enough, and ν . The integrable system is described by two dimensionless parameters: $\lambda = mL^2\omega_{\perp}/\hbar$, characterizing the aspect ratio, and the scaled vector potential $l_0 = LA/(2\pi)$. In the calculations, $\lambda = \pi^3(1 + \sqrt{5}) \approx 100$ and $l_0 = 0.25 - e^{-4} \approx 0.232$ are expressed in terms of transcendental numbers. Approximately the same results are obtained for any $l_0 > 0.01$. In Fig. 3(a) and (c), $V_{s'} = 10^6 V_0$ for all scatterers is in the unitary regime ($V_0 = 2\pi\hbar^{5/2}m^{-3/2}\omega_{\perp}^{-1/2}$ is the scale of the interaction strength). Approximately the same results are obtained for any $V_{s'} > V_0$. In Fig. 3(b), $V_{s'}/V_0 = 10^6, 10^{-1}, 10^{-2}, 2 \times 10^{-3}, 10^{-3}, 10^{-4}, 0$ for the 6 IPR values from left to right.

The Lorentzian width is related to NPC as $\Gamma_s/\Delta E = \eta_s^{-1}/(2\pi)$. Figure 3(a) demonstrates the linear dependence even when $\eta_s^{-1} < 2\pi$. Therefore, even when the Fermi golden rule is inapplicable to Γ_s as $\Gamma_s/\Delta E < 1$, the strength function can be approximated by the Lorentzian profile.

The physical implication of the rule (4) is related to the fluctuations of expectation values $\langle \alpha | \hat{A} | \alpha \rangle$ of an observable \hat{A} , characterized by their variance $\text{Var}_{\alpha}(\hat{A}) =$

$\overline{\langle \alpha | \hat{A} | \alpha \rangle^2} - \overline{\langle \alpha | \hat{A} | \alpha \rangle}^2$ over the eigenstates $|\alpha\rangle$. It is proportional to IPR and the variance for the underlying integrable system

$$\text{Var}_\alpha(\hat{A}) = \eta \text{Var}_n(\hat{A}) \quad (7)$$

as was derived, in slightly different form, in [28]. This relation can also be derived in the same way as the relation between the initial, thermal, and relaxed expectation values (7) in [24] replacing the density matrix by the observable. Then (7), like the relation (7) in [24], is applicable to perturbations with no selection rules. The relation (7) was compared with numerical results [28] for a many-body system with two-body interactions. However, such systems do have selection rules, as each two-body interaction conserves quantum numbers of other particles. It is probably the reason why the numerical results [28] were described by (7) only up to some energy-dependent factor. Systems with separable perturbations have no selection rules, and the relation (7) describes the dependence of variances on the number of scatterers and interaction strength for four observables [see Fig. 3 (b) and (c)]. The observables are: the axial momentum $\langle nl | \hat{p}_{ax} | n'l' \rangle = l \delta_{n'n} \delta_{l'l}$, the occupation of positive momenta $\langle nl | \hat{P}_{pos} | n'l' \rangle = \delta_{n'n} \delta_{l'l} \theta(l)$, the occupation of the odd axial modes $\langle nl | \hat{P}_{odd} | n'l' \rangle = \delta_{n'n} \delta_{l'l} \delta_{l\%2,1}$, and the part of the transverse potential energy $m\omega_\perp^2 \rho^2/2$ in the total energy, $\langle nl | \hat{U} | n'l' \rangle = [(2n+1)\delta_{n'n} - (n+1)\delta_{n'n+1} - n\delta_{n'n-1}] \delta_{l'l} \hbar\omega_\perp / (2E_{nl})$. The averages and variances of these observable expectation values over the integrable system eigenstates are directly calculated. The averages are $\overline{\langle nl | \hat{p}_{ax} | nl \rangle} = l_0$, $\overline{\langle nl | \hat{P}_{pos} | nl \rangle} = 1/2$, $\overline{\langle nl | \hat{P}_{odd} | nl \rangle} = 1/2$, and $\overline{\langle nl | \hat{U} | nl \rangle} = 1/3$. Although the average expectation value of the axial momentum is constant, its variation amplitude increases with the state energy. Then, the variance $\text{Var}_{nl}(p_{ax}) = mL^2(E_{max}^{5/2} - E_{min}^{5/2})/[10\pi^2\hbar(E_{max}^{3/2} - E_{min}^{3/2})]$ depends on the averaging interval $[E_{min}, E_{max}]$ boundaries. The variances for other observables are independent of the interval, $\text{Var}_{nl}(\hat{P}_{pos}) = 1/4$, $\text{Var}_{nl}(\hat{P}_{odd}) = 1/4$, and $\text{Var}_{nl}(\hat{U}) = 1/45$.

Together with (4), the relation (7) provides the decay of fluctuation variance on the increase of the number of scatterers, $\text{Var}_\alpha(\hat{A}) = \text{Var}_n(\hat{A})/[\eta_2^{-1} + (s-2)\nu]$, or eigenstate thermalization approaching in a single-body system. Then, a set of fixed scatterers mimics the behavior of many-body systems — sets of moving scatterers. The fluctuation decay is only inversely proportional to the number of fixed scatterers, i.e., much slower than the exponential decay in many-body systems. This opens possibilities of fine control of the system chaoticity and exploration of the integrability-chaos crossover.

Chaotic properties of many-body systems of inter-

acting particles are studied in numerous experimental and theoretical researches. However, due to computational difficulties, a direct numerical simulation is performed for lattice systems (e.g., [13, 16, 18, 27–29, 33, 34, 36, 37, 39, 42, 43]) with a finite Hilbert space, while the problem complexity increases as a high power of the lattice site number and exponentially with the number of particles. A single particle in an external potential allows us to explore an infinite Hilbert space. Eigenstate thermalization has been analyzed [57] for 3×10^4 states of a Sinai-type billiard. However, the chaoticity of that system can not be tuned and the calculation of highly excited states is obstructed by the increase of the coordinate grid size. The properties of systems with several independent perturbations (particularly, scatterers) can be tuned by the number of perturbations and their strengths. Although the general results are confirmed by numerical calculations for a specific model, they are applicable to any integrable system, perturbed by several scatterers.

The predictions should be testable experimentally in several physical systems. Tightly-trapped cold atoms of one kind can play the role of scatterers for an atom of a second kind in a wide trap. Moreover, several atoms of the second kind — with interactions between them turned off by a broad Feshbach resonance — can be used to get averages. In optics, photons in a cavity can be scattered by optical defects [58].

-
- [1] T. Kinoshita, T. Wenger, and D. S. Weiss, A quantum Newton's cradle, *Nature* **440**, 900 (2006).
 - [2] Y. Tang, W. Kao, K.-Y. Li, S. Seo, K. Mallayya, M. Rigol, S. Gopalakrishnan, and B. L. Lev, Thermalization near integrability in a dipolar quantum Newton's cradle, *Phys. Rev. X* **8**, 021030 (2018).
 - [3] A. Di Carli, C. D. Colquhoun, G. Henderson, S. Flannigan, G.-L. Oppo, A. J. Daley, S. Kuhr, and E. Haller, Excitation modes of bright matter-wave solitons, *Phys. Rev. Lett.* **123**, 123602 (2019).
 - [4] D. Luo, Y. Jin, J. H. V. Nguyen, B. A. Malomed, O. V. Marchukov, V. A. Yurovsky, V. Dunjko, M. Olshanii, and R. G. Hulet, Creation and characterization of matter-wave breathers, *Phys. Rev. Lett.* **125**, 183902 (2020).
 - [5] I. Mazets, Integrability breakdown in longitudinally trapped, one-dimensional bosonic gases, *Eur. Phys. J. D* **65**, 43 (2011).
 - [6] G. P. Brandino, J.-S. Caux, and R. M. Konik, Glimmers of a quantum KAM theorem: Insights from quantum quenches in one-dimensional Bose gases, *Phys. Rev. X* **5**, 041043 (2015).
 - [7] V. A. Yurovsky, B. A. Malomed, R. G. Hulet, and M. Olshanii, Dissociation of one-dimensional matter-wave breathers due to quantum many-body effects, *Phys. Rev. Lett.* **119**, 220401 (2017).
 - [8] O. V. Marchukov, B. A. Malomed, V. Dunjko, J. Ruhl, M. Olshanii, R. G. Hulet, and V. A. Yurovsky, Quantum

- fluctuations of the center of mass and relative parameters of nonlinear Schrödinger breathers, *Phys. Rev. Lett.* **125**, 050405 (2020).
- [9] N. L. Harshman, M. Olshanii, A. S. Dehkharghani, A. G. Volosniev, S. G. Jackson, and N. T. Zinner, Integrable families of hard-core particles with unequal masses in a one-dimensional harmonic trap, *Phys. Rev. X* **7**, 041001 (2017).
- [10] J. M. Deutsch, Quantum statistical mechanics in a closed system, *Phys. Rev. A* **43**, 2046 (1991).
- [11] M. Srednicki, Chaos and quantum thermalization, *Phys. Rev. E* **50**, 888 (1994).
- [12] M. Rigol, V. Dunjko, and M. Olshanii, Thermalization and its mechanism for generic isolated quantum systems, *Nature* **452**, 854 (2008).
- [13] A. Khodja, R. Steinigeweg, and J. Gemmer, Relevance of the eigenstate thermalization hypothesis for thermal relaxation, *Phys. Rev. E* **91**, 012120 (2015).
- [14] A. M. Kaufman, M. E. Tai, A. Lukin, M. Rispoli, R. Schittko, P. M. Preiss, and M. Greiner, Quantum thermalization through entanglement in an isolated many-body system, *Science* **353**, 794 (2016).
- [15] J. M. Deutsch, Eigenstate thermalization hypothesis, *Reps. Progr. Phys.* **81**, 082001 (2018).
- [16] M. Rigol, V. Dunjko, V. Yurovsky, and M. Olshanii, Relaxation in a completely integrable many-body quantum system: An ab initio study of the dynamics of the highly excited states of 1D lattice hard-core Bosons, *Phys. Rev. Lett.* **98**, 050405 (2007).
- [17] E. V. H. Doggen and J. J. Kinnunen, Quench-induced delocalization, *New J. Phys.* **16**, 113051 (2014).
- [18] S. Nandy, A. Sen, A. Das, and A. Dhar, Eigenstate gibbs ensemble in integrable quantum systems, *Phys. Rev. B* **94**, 245131 (2016).
- [19] W. Verstraelen, D. Sels, and M. Wouters, Unitary work extraction from a generalized gibbs ensemble using bragg scattering, *Phys. Rev. A* **96**, 023605 (2017).
- [20] C.-H. Wu, Time evolution and thermodynamics for a nonequilibrium system in phase-space, *Can. J. Phys.* **97**, 609 (2019).
- [21] W. G. Brown, L. F. Santos, D. J. Starling, and L. Viola, Quantum chaos, delocalization, and entanglement in disordered heisenberg models, *Phys. Rev. E* **77**, 021106 (2008).
- [22] V. A. Yurovsky and M. Olshanii, Restricted thermalization for two interacting atoms in a multimode harmonic waveguide, *Phys. Rev. A* **81**, 043641 (2010).
- [23] C. Stone, Y. A. E. Aoud, V. A. Yurovsky, and M. Olshanii, Two simple systems with cold atoms: quantum chaos tests and non-equilibrium dynamics, *New J. Phys.* **12**, 055022 (2010).
- [24] V. A. Yurovsky and M. Olshanii, Memory of the initial conditions in an incompletely chaotic quantum system: Universal predictions with application to cold atoms, *Phys. Rev. Lett.* **106**, 025303 (2011).
- [25] V. A. Yurovsky, A. Ben-Reuven, and M. Olshanii, Dynamics of relaxation and fluctuations of the equilibrium state in an incompletely chaotic system, *J. Phys. Chem. B* **115**, 5340 (2011).
- [26] M. Kollar, F. A. Wolf, and M. Eckstein, Generalized gibbs ensemble prediction of prethermalization plateaus and their relation to nonthermal steady states in integrable systems, *Phys. Rev. B* **84**, 054304 (2011).
- [27] M. Olshanii, K. Jacobs, M. Rigol, V. Dunjko, H. Kennard, and V. A. Yurovsky, An exactly solvable model for the integrability-chaos transition in rough quantum billiards, *Nature Communications* **3**, 641 (2012).
- [28] C. Neuenhahn and F. Marquardt, Thermalization of interacting fermions and delocalization in Fock space, *Phys. Rev. E* **85**, 060101(R) (2012).
- [29] E. Canovi, D. Rossini, R. Fazio, G. E. Santoro, and A. Silva, Many-body localization and thermalization in the full probability distribution function of observables, *New J. Phys.* **14**, 095020 (2012).
- [30] J. Larson, B. M. Anderson, and A. Altland, Chaos-driven dynamics in spin-orbit-coupled atomic gases, *Phys. Rev. A* **87**, 013624 (2013).
- [31] L. Campos Venuti, S. Yeshwanth, and S. Haas, Equilibration times in clean and noisy systems, *Phys. Rev. A* **87**, 032108 (2013).
- [32] O. Fialko, Decoherence via coupling to a finite quantum heat bath, *J. Phys. B* **47**, 045302 (2014).
- [33] F. Andraschko, T. Enss, and J. Sirker, Purification and many-body localization in cold atomic gases, *Phys. Rev. Lett.* **113**, 217201 (2014).
- [34] C. Khripkov, A. Vardi, and D. Cohen, Quantum thermalization: anomalous slow relaxation due to percolation-like dynamics, *New J. Phys.* **17**, 023071 (2015).
- [35] L. C. Venuti and P. Zanardi, Theory of temporal fluctuations in isolated quantum systems, *Int. J. Mod. Phys. B* **29**, 1530008 (2015).
- [36] C. Khripkov, D. Cohen, and A. Vardi, Thermalization of bipartite Bose-Hubbard models, *J. Phys. Chem. A* **120**, 3136 (2016).
- [37] C. Bartsch and J. Gemmer, Necessity of eigenstate thermalisation for equilibration towards unique expectation values when starting from generic initial states, *Europhys. Lett.* **118**, 10006 (2017).
- [38] C. B. Dağ, S.-T. Wang, and L.-M. Duan, Classification of quench-dynamical behaviors in spinor condensates, *Phys. Rev. A* **97**, 023603 (2018).
- [39] F. Iglói, B. Blaß, G. m. H. Roósz, and H. Rieger, Quantum XX model with competing short- and long-range interactions: Phases and phase transitions in and out of equilibrium, *Phys. Rev. B* **98**, 184415 (2018).
- [40] T. Goldfriend and J. Kurchan, Equilibration of quasi-integrable systems, *Phys. Rev. E* **99**, 022146 (2019).
- [41] A. Bastianello, Lack of thermalization for integrability-breaking impurities, *Europhys. Lett.* **125**, 20001 (2019).
- [42] W.-J. Huang, Y.-B. Wu, G.-C. Guo, and X.-B. Zou, Ergodic-nonergodic transition with cold spinless fermions in a cavity, *Phys. Rev. A* **105**, 033315 (2022).
- [43] J.-L. Ma, Q. Li, and L. Tan, Ergodic and nonergodic phases in a one-dimensional clean Jaynes-Cummings-Hubbard system with detuning, *Phys. Rev. B* **105**, 165432 (2022).
- [44] B. Georgeot and D. L. Shepelyansky, Breit-Wigner width and inverse participation ratio in finite interacting Fermi systems, *Phys. Rev. Lett.* **79**, 4365 (1997).
- [45] See Supplemental Material for derivation details.
- [46] M. V. Berry, Regular and irregular semiclassical wavefunctions, *J. Phys. A* **10**, 2083 (1977).
- [47] E. P. Wigner, Characteristic vectors of bordered matrices with infinite dimensions, *Ann. Math* **62**, 548 (1955).
- [48] Y. V. Fyodorov and A. D. Mirlin, Statistical properties of random banded matrices with strongly fluctuating diagonal elements, *Phys. Rev. B* **52**, R11580 (1995).
- [49] K. Frahm and A. Müller-Groeling, Analytical results for

- random band matrices with preferential basis, Europhys. Lett. **32**, 385 (1995).
- [50] P. Jacquod and D. L. Shepelyansky, Hidden Breit-Wigner distribution and other properties of random matrices with preferential basis, Phys. Rev. Lett. **75**, 3501 (1995).
- [51] P. Šeba, Wave chaos in singular quantum billiard, Phys. Rev. Lett. **64**, 1855 (1990).
- [52] T. Cheon and T. Shigehara, Scale anomaly and quantum chaos in billiards with pointlike scatterers, Phys. Rev. E **54**, 3300 (1996).
- [53] O. Legrand, F. Mortessagne, and R. L. Weaver, Semiclassical analysis of spectral correlations in regular billiards with point scatterers, Phys. Rev. E **55**, 7741 (1997).
- [54] N. Yesha, Uniform distribution of eigenstates on a torus with two point scatterers, J. Spectr. Theory **8**, 1509 (2018).
- [55] Q. Guan, V. Klinkhamer, R. Klemt, J. H. Becher, A. Bergschneider, P. M. Preiss, S. Jochim, and D. Blume, Density oscillations induced by individual ultracold two-body collisions, Phys. Rev. Lett. **122**, 083401 (2019).
- [56] K. Kanjilal, J. L. Bohn, and D. Blume, Pseudopotential treatment of two aligned dipoles under external harmonic confinement, Phys. Rev. A **75**, 052705 (2007).
- [57] A. H. Barnett, Asymptotic rate of quantum ergodicity in chaotic euclidean billiards, Comm. Pure Appl. Math. **59**, 1457 (2006).
- [58] R. Bruck, C. Liu, O. L. Muskens, A. Fratalocchi, and A. Di Falco, Ultrafast all-optical order-to-chaos transition in silicon photonic crystal chips, Las. Phot. Rev. **10**, 688 (2016).

**SUPPLEMENTAL MATERIAL FOR:
EXPLORING INTEGRABILITY-CHAOS TRANSITION WITH A SEQUENCE OF INDEPENDENT
PERTURBATIONS**

Numbers of equations in the Supplemental material are started from S. References to equations in the Letter do not contain S.

Averages

The microcanonical window $[E_{min}, E_{max}]$, containing a large number of states \mathcal{N}_{MC} , is small compared to the system energy scales. The microcanonical average is defined as

$$\overline{F(\alpha)}^\alpha = \frac{1}{\mathcal{N}_{MC}} \sum_{\alpha \in MC} F(\alpha), \quad (\text{S-1})$$

where $\alpha \in MC$ means that $E_{min} < E_\alpha < E_{max}$.

The average over states with a fixed energy difference in the strength function (1) is defined as

$$\langle F(\alpha, \beta) \rangle = \frac{1}{\mathcal{N}_{MC}} \sum_{\alpha', \beta' \in MC} F(\alpha', \beta') \bar{\delta}_{E_\beta - E_\alpha + E_{\alpha'}, E_{\beta'}}, \quad (\text{S-2})$$

where $\bar{\delta}_{E_\beta - E_\alpha + E_{\alpha'}, E_{\beta'}}$ selects the state β' with the energy $E_{\beta'}$ closest to $E_\beta - E_\alpha + E_{\alpha'}$.

Derivation of the relation (2)

Consider at first the Hamiltonian $\hat{H}_2 = \hat{H}_0 + \hat{V}_1 + \hat{V}_2$. The Schrödinger equations lead to the following relations between the eigenstates $|\alpha_2\rangle$, $|\alpha_1\rangle$, and $|\mathbf{n}\rangle$ of the Hamiltonians \hat{H}_2 , \hat{H}_1 , and \hat{H}_0 , respectively,

$$\langle \alpha_1 | \alpha_2 \rangle = \frac{\langle \alpha_1 | \hat{V}_2 | \alpha_2 \rangle}{E_{\alpha_2} - E_{\alpha_1}}, \quad \langle \mathbf{n} | \alpha_1 \rangle = \frac{\langle \mathbf{n} | \hat{V}_1 | \alpha_1 \rangle}{E_{\alpha_1} - E_{\mathbf{n}}} \quad (\text{S-3})$$

Let us represent the expansion coefficients as $\langle \mathbf{n}|\alpha_2\rangle = \sum_{\alpha_1} \langle \mathbf{n}|\alpha_1\rangle \langle \alpha_1|\alpha_2\rangle$ and separate the diagonal part of the strength function (1)

$$W_2^{diag}(E_{\mathbf{n}}, E_{\alpha_2}) = \left\langle \sum_{\alpha_1} |\langle \mathbf{n}|\alpha_1\rangle|^2 |\langle \alpha_1|\alpha_2\rangle|^2 \right\rangle \\ = \frac{1}{\mathcal{N}_{MC}} \sum_{E_{\alpha_1}} \sum_{\mathbf{n}', \alpha'_1 \in MC} |\langle \mathbf{n}'|\alpha'_1\rangle|^2 \bar{\delta}_{E_{\alpha_1} - E_{\mathbf{n}} + E_{\mathbf{n}'}, E_{\alpha'_1}} \sum_{\alpha'_2} \frac{|\langle \alpha'_1|\hat{V}_2|\alpha'_2\rangle|^2}{(E_{\alpha_2} - E_{\alpha_1})^2} \bar{\delta}_{E_{\alpha_2} - E_{\alpha_1} + E_{\alpha'_1}, E_{\alpha'_2}}. \quad (\text{S-4})$$

The eigenstate $|\alpha'_1\rangle$ is independent of the potential \hat{V}_2 . Then, the last summand can be approximated by its microcanonical average over α'_1 , leading to

$$W_2^{diag}(E_{\mathbf{n}}, E_{\alpha_2}) \approx \sum_{E_{\alpha_1}} W_1(E_{\mathbf{n}}, E_{\alpha_1}) \left\langle |\langle \alpha_1|\alpha_2\rangle|^2 \right\rangle. \quad (\text{S-5})$$

If the non-diagonal part of the strength function can be neglected, replacing α_2 , α_1 , \hat{V}_2 , and \hat{V}_1 by α_s , α_{s-1} , \hat{V}_s , and $\sum_{s'=1}^{s-1} \hat{V}_{s'}$, respectively, we get the relation (2).

In order to evaluate the non-diagonal part, let us represent the expansion coefficients as

$$\langle \mathbf{n}|\alpha_2\rangle = \frac{1}{E_{\alpha_2} - E_{\mathbf{n}}} \sum_{\alpha_1} \left(\langle \mathbf{n}|\hat{V}_1|\alpha_1\rangle \langle \alpha_1|\alpha_2\rangle + \langle \mathbf{n}|\alpha_1\rangle \langle \alpha_1|\hat{V}_2|\alpha_2\rangle \right)$$

using Eqs. (S-3) and the completeness of the set $|\alpha_1\rangle$ [α_1 here is the same as in (S-4)]. The corresponding probabilities can be expressed

$$|\langle \mathbf{n}|\alpha_2\rangle|^2 = \frac{1}{(E_{\alpha_2} - E_{\mathbf{n}})^2} \sum_{\alpha_1, \alpha'_1} \left(B_{\alpha_1\alpha'_1}(\hat{V}_1, \hat{V}_1, \mathbf{n}) B_{\alpha'_1\alpha_1}(\hat{I}, \hat{I}, \alpha_2) + B_{\alpha_1\alpha'_1}(\hat{I}, \hat{I}, \mathbf{n}) B_{\alpha'_1\alpha_1}(\hat{V}_2, \hat{V}_2, \alpha_2) \right. \\ \left. + B_{\alpha_1\alpha'_1}(\hat{I}, \hat{V}_1, \mathbf{n}) B_{\alpha'_1\alpha_1}(\hat{I}, \hat{V}_2, \alpha_2) + B_{\alpha_1\alpha'_1}(\hat{V}_1, \hat{I}, \mathbf{n}) B_{\alpha'_1\alpha_1}(\hat{V}_2, \hat{I}, \alpha_2) \right) \quad (\text{S-6})$$

in terms of the products of the matrix elements

$$B_{\alpha_1\alpha'_1}(\hat{O}_1, \hat{O}_2, \beta) = \langle \alpha_1|\hat{O}_1|\beta\rangle \langle \beta|\hat{O}_2|\alpha'_1\rangle.$$

In the generic case, different degrees of freedom of \hat{H}_0 have incommensurate frequencies, and the quantum numbers \mathbf{n} and \mathbf{n}' of the energy-neighboring states will be mutually uncorrelated. Then, substituting (S-6) into the strength function (1), we can replace $B_{\alpha_1\alpha'_1}(\hat{O}_1, \hat{O}_2, \mathbf{n})$ by its microcanonical average $\overline{B_{\alpha_1\alpha'_1}(\hat{O}_1, \hat{O}_2, \mathbf{n})}$ [see (S-1)] and obtain the following approximation for the fixed energy difference average [see (S-2)]

$$\left\langle \frac{1}{(E_{\alpha_2} - E_{\mathbf{n}})^2} B_{\alpha_1\alpha'_1}(\hat{O}_1, \hat{O}_2, \mathbf{n}) B_{\alpha'_1\alpha_1}(\hat{O}_3, \hat{O}_4, \alpha_2) \right\rangle \approx \frac{1}{(E_{\alpha_2} - E_{\mathbf{n}})^2} \overline{B_{\alpha_1\alpha'_1}(\hat{O}_1, \hat{O}_2, \mathbf{n}) B_{\alpha'_1\alpha_1}(\hat{O}_3, \hat{O}_4, \alpha_2)}^{\alpha_2} \quad (\text{S-7})$$

The independence of the random functions $\langle \mathbf{n}|\alpha_s\rangle$ and $\langle \mathbf{n}|\alpha'_s\rangle$ for $\alpha_s \neq \alpha'_s$ [11, 46] leads to the approximate equality of the microcanonical averages

$$\overline{|\alpha_s\rangle \langle \alpha_s|^{\alpha_s}} \approx \overline{|\mathbf{n}\rangle \langle \mathbf{n}|}^{\mathbf{n}} \quad (\text{S-8})$$

of the product of two eigenfunctions. This results in

$$\overline{B_{\alpha_1\alpha'_1}(\hat{I}, \hat{I}, \beta)}^{\beta} \approx \frac{1}{\mathcal{N}_{MC}} \delta_{\alpha_1\alpha'_1}, \quad \overline{B_{\alpha_1\alpha'_1}(\hat{I}, \hat{V}, \beta)}^{\beta} \approx \frac{1}{\mathcal{N}_{MC}} \langle \alpha_1|\hat{V}|\alpha'_1\rangle \quad (\text{S-9})$$

if α_1 and α'_1 belong to the microcanonical interval (otherwise, the averages vanish). Then, using Eqs. (S-6), (S-7), (S-8), and (S-9) one can approximate the diagonal and non-diagonal parts of the strength function (1) as

$$W_2^{diag}(E_{\mathbf{n}}, E_{\alpha_2}) \approx \frac{1}{\mathcal{N}_{MC}^2 (E_{\alpha_2} - E_{\mathbf{n}})^2} \left[\sum_{\mathbf{n}, \mathbf{n}' \in MC} \left(|\langle \mathbf{n}|\hat{V}_1|\mathbf{n}'\rangle|^2 + |\langle \mathbf{n}|\hat{V}_2|\mathbf{n}'\rangle|^2 \right) + 2 \sum_{\alpha_1 \in MC} \langle \alpha_1|\hat{V}_1|\alpha_1\rangle \langle \alpha_1|\hat{V}_2|\alpha_1\rangle \right] \quad (\text{S-10})$$

$$W_2^{non\text{d}}(E_{\mathbf{n}}, E_{\alpha_2}) \approx \frac{2}{\mathcal{N}_{MC}^2(E_{\alpha_2} - E_{\mathbf{n}})^2} \left(\sum_{\mathbf{n}, \mathbf{n}' \in MC} \langle \mathbf{n} | \hat{V}_1 | \mathbf{n}' \rangle \langle \mathbf{n}' | \hat{V}_2 | \mathbf{n} \rangle - \sum_{\alpha_1 \in MC} \langle \alpha_1 | \hat{V}_1 | \alpha_1 \rangle \langle \alpha_1 | \hat{V}_2 | \alpha_1 \rangle \right).$$

The last, single, summations here can be neglected compared to the double summations. Then, the non-diagonal part is negligible when the condition (3) for $s = 2$ is satisfied. The recurrent application of this condition provides the condition (3) for any s .

The microcanonical average of the product of two eigenfunctions is the Berry autocorrelation function [46]

$$\overline{\langle \mathbf{R} - \mathbf{r}/2 | \mathbf{n} \rangle \langle \mathbf{n} | \mathbf{R} + \mathbf{r}/2 \rangle}^{\mathbf{n}} \approx \Gamma(D/2) \frac{J_{D/2-1}(K(\mathbf{R})r)}{(K(\mathbf{R})r/2)^{D/2-1}},$$

where Γ is the Γ -function, D is the number of degrees of freedom (the dimension of the vectors \mathbf{n} , \mathbf{r} , and \mathbf{R}), J is the Bessel function, and $K(\mathbf{R})$ is the absolute value of the local wavevector. The autocorrelation function decays when r exceeds the characteristic de Broglie wavelength K^{-1} , determined by the mean energy of the microcanonical interval. Then, $W_2^{non\text{d}}$ becomes negligible when the local coordinate-dependent potentials \hat{V}_1 and \hat{V}_2 are separated spatially by more than the characteristic de Broglie wavelength.

Equation (S-10) also shows that $W_s(E_{\mathbf{n}}, E_{\alpha_s})$ should decay as $(E_{\mathbf{n}} - E_{\alpha_s})^{-2}$ in the limit $|E_{\mathbf{n}} - E_{\alpha_s}| \rightarrow \infty$.

Derivation of the recurrent relation (5) for NPC

Choosing the Lorentzian profile (4) for the continuous strength function $W_s(E_{\mathbf{n}}, E_{\alpha_s}) \approx W_L(E_{\alpha_s} - E_{\mathbf{n}}, \Gamma_s) \Delta E$, replacing the sum over $E_{\alpha_{s-1}}$ by the integral, and substituting $\langle |\langle \alpha_s | \alpha_{s-1} \rangle|^2 \rangle = W'(E_{\alpha_s}, E_{\alpha_{s-1}}) \Delta E$, we reduce (2) to the integral equation:

$$W_L(E_{\alpha_s} - E_{\mathbf{n}}, \Gamma_s) = C_{SI} \int dE_{\alpha_{s-1}} W'(E_{\alpha_s}, E_{\alpha_{s-1}}) W_L(E_{\alpha_{s-1}} - E_{\mathbf{n}}, \Gamma_{s-1}), \quad (\text{S-11})$$

where the factor C_{SI} compensates for inaccuracy of the sum-integral replacement. The solution of (S-11) $W'(E_{\alpha_s}, E_{\alpha_{s-1}}) = W_L(E_{\alpha_s} - E_{\alpha_{s-1}}, \Gamma')$ with $\Gamma' = \Gamma_s - \Gamma_{s-1}$ is obtained using the Fourier transform.

Whenever it is applicable, the Fermi golden rule provides [27, 47–50]

$$\Gamma_s \approx \frac{\pi}{\mathcal{N}_{MC}^2 \Delta E} \sum_{\mathbf{n}, \mathbf{n}' \in MC} \left| \left\langle \mathbf{n} \left| \sum_{s'=1}^s \hat{V}_{s'} \right| \mathbf{n}' \right\rangle \right|^2.$$

For independent perturbations, obeying the condition (3), the sum over \mathbf{n} and \mathbf{n}' above can be split as

$$\sum_{\mathbf{n}, \mathbf{n}' \in MC} \left| \left\langle \mathbf{n} \left| \sum_{s'=1}^s \hat{V}_{s'} \right| \mathbf{n}' \right\rangle \right|^2 = \sum_{\mathbf{n}, \mathbf{n}' \in MC} \left| \left\langle \mathbf{n} \left| \sum_{s'=1}^{s-1} \hat{V}_{s'} \right| \mathbf{n}' \right\rangle \right|^2 + \sum_{\mathbf{n}, \mathbf{n}' \in MC} \left| \langle \mathbf{n} | \hat{V}_s | \mathbf{n}' \rangle \right|^2.$$

Then $\Gamma_s = \Gamma_{s-1} + \Gamma'$, in the agreement with the general relation derived above.

For the Lorentzian profile IPR can be approximated as $\eta_s \equiv \sum_{\mathbf{n}} |\langle \alpha_s | \mathbf{n} \rangle|^4 \approx \int dE_{\mathbf{n}} W_L^2(E_{\alpha_s} - E_{\mathbf{n}}, \Gamma_s) \Delta E = \Delta E / (2\pi\Gamma_s)$. This leads to the relation for NPC (5) with $\nu = 2\pi\Gamma' / \Delta E$. For large s the chaotic properties of $|\alpha_s\rangle$ weakly depend on s and if the shape of \hat{V}_s is independent of s (as for scatterers with the same strength), ν will be approximately independent of s .